Clinical Anatomy 00:00–00 (2014)

ORIGINAL COMMUNICATION

Nasal Airway and Septal Variation in Unilateral and Bilateral Cleft Lip and Palate

JOHN M. STARBUCK,[1*] MICHAEL T. FRIEL,[2] AHMED GHONEIMA,[1] ROBERTO L. FLORES,[3] SUNIL THOLPADY,[3] AND KATHERINE KULA[1]

[1]*Department of Orthodontics and Oral Facial Genetics, School of Dentistry, Indiana University, Indianapolis, Indiana 46202*

[2]*Division of Plastic Surgery, Department of Surgery, University of Mississippi Medical Center, Jackson, Mississippi 39126*

[3]*Division of Plastic Surgery, Department of Surgery, Indiana University, Indianapolis, Indiana 46202*

Cleft lip and palate (CLP) affects the dentoalveolar and nasolabial facial regions. Internal and external nasal dysmorphology may persist in individuals born with CLP despite surgical interventions. 7–18 year old individuals born with unilateral and bilateral CLP ($n = 50$) were retrospectively assessed using cone beam computed tomography. Anterior, middle, and posterior nasal airway volumes were measured on each facial side. Septal deviation was measured at the anterior and posterior nasal spine, and the midpoint between these two locations. Data were evaluated using principal components analysis (PCA), multivariate analysis of variance (MANOVA), and post-hoc ANOVA tests. PCA results show partial separation in high dimensional space along PC1 (48.5% variance) based on age groups and partial separation along PC2 (29.8% variance) based on CLP type and septal deviation patterns. MANOVA results indicate that age ($P = 0.007$) and CLP type ($P \leq 0.001$) significantly affect nasal airway volume and septal deviation. ANOVA results indicate that anterior nasal volume is significantly affected by age ($P \leq 0.001$), whereas septal deviation patterns are significantly affected by CLP type ($P \leq 0.001$). Age and CLP type affect nasal airway volume and septal deviation patterns. Nasal airway volumes tend to be reduced on the clefted sides of the face relative to non-clefted sides of the face. Nasal airway volumes tend to strongly increase with age, whereas septal deviation values tend to increase only slightly with age. These results suggest that functional nasal breathing may be impaired in individuals born with the unilateral and bilateral CLP deformity. Clin. Anat. 00:000–000, 2014.

Key words: cone beam computed tomography; nose deformity; craniofacial morphology; three-dimensional (3D) imaging; growth and development; nasal obstruction

INTRODUCTION

Human faces are highly variable and distinctive due to factors such as ethnic background, genetic makeup, environmental influences, age, sex, body weight, and the presence or absence of congenital anomalies (Farkas et al., 1992; Ferrario et al., 1998; Starbuck and Ward, 2007; Klimentidis and Shriver, 2009). Facial morphogenesis follows an embryonic blueprint or 'bauplan' whereby the frontal, nasal, maxillary, and mandibular facial prominences are guided by spatiotemporal and morphogenetic developmental

Contract grant sponsor: Indiana University-Purdue University Indianapolis (IUPUI) Signature Center Initiative-Three Dimensional Imaging of the Craniofacial Complex Center (3D ICCC); Jarabak Endowed Professorship.

*Correspondence to: John Starbuck; Department of Orthodontics and Facial Genetics, Indiana University School of Dentistry, 1121 W. Michigan St. DS 250D, Indianapolis, IN 46202, USA. E-mail: jstarbuc@iu.edu

Received 28 April 2014; Revised 29 May 2014; Accepted 3 June 2014

Published online in Wiley Online Library (wileyonlinelibrary.com). DOI: 10.1002/ca.22428

mechanisms to form, grow, and fuse in a highly coordinated fashion to ultimately produce a normal, functional facial complex (Brugmann et al., 2006; Jiang et al., 2006; Feng et al., 2009). Deviation of craniofacial prominences from this facial arrangement due to genetic, environmental, and developmental perturbations is selected against due to the increased probability of the formation of congenital facial anomalies and spontaneous abortion (Young et al., 2014). The development, growth, and fusion of each individual craniofacial prominence is affected by specific combinations of protein coding genes, gene copy number variation, and regulatory enhancers (Attanasio et al., 2013). When craniofacial prominences fail to fuse correctly a large gap or "cleft" between facial elements can arise or entire facial regions can be missing (Young et al., 2000).

Cleft lip and palate (CLP) is a relatively common unilateral or bilateral congenital facial deformity that occurs during facial morphogenesis when the nasal and maxillary facial prominences fail to fuse correctly around the 36th or 37th day of gestation (Thomason and Dixon, 2009; Weinberg et al., 2009; Lee et al., 2012; Marazita, 2012; Choi et al., 2013). CLP has been found in ancient populations and has likely occurred throughout human existence (Gregg et al., 1981). CLP can impair breathing, swallowing, and mastication (Bugaighis et al., 2013). Facial traits typically associated with CLP include a clefted lip and palate, midfacial hypoplasia, a deviated anterior nasal spine, a distorted nasal septum, reduced nasal chamber width, an inferiorly positioned nasal border, and asymmetry of the maxilla, mandible, and nasolabial regions of the face (Harvold, 1953; Molsted and Dahl, 1990; Ras et al., 1994; Ras et al., 1995; Son, 1995; Kolbenstvedt et al., 2002; Suri et al., 2008; Jena et al., 2011; Agarwal et al., 2012; Bell et al., 2013; Bugaighis et al., 2013; Choi et al., 2013; Freeman et al., 2013; Hasanzadeh et al., 2014). Surgical repair of the primary cutaneous upper lip is usually carried out around 2–3 months of age, whereas surgical repair of the hard palate is generally carried out around 6–12 months of age (Kolbenstvedt et al., 2002; Marazita, 2012). Some individuals born with CLP require an alveolar bone graft during the mixed dentition stage of growth (7–11 years) to provide bone tissue for the clefted dentoalveolus to unite the maxillary segments and provide skeletal support for canine eruption (Kolbenstvedt et al., 2002; Trindade-Suedam et al., 2012). Individuals with CLP commonly have septal deviation due to (1) unilateral attachment of the orbicularis oris to the anterior caudal septum on the non-affected side, (2) unilateral attachment of the vomer secondary to clefting of the hard palate, (3) lateral deviation of the lower and middle vault secondary to unopposed action of the zygomaticus major and minor on the alar base, and (4) compounded scoliosis of the septum, lower and middle vault secondary to deviation of the greater and lesser segments of the alveolus (Hall and Precious, 2012). Surgically repaired faces often exhibit iatrogenic scarring and facial asymmetries that contribute to stigmata (Seidenstricker-Kink et al., 2008; Choi et al., 2013; Freeman et al., 2013).

Cone beam computed tomography (CBCT) high resolution three-dimensional images can be quickly acquired with low radiation doses and are a useful diagnostic tool for measuring craniofacial variation (Tso et al., 2009; Schendel and Hatcher, 2010; Trindade-Suedam et al., 2012). CBCT images and appropriate imaging software hold many advantages over traditional two-dimensional cephalograms because they allow three-dimensional measurement of anatomical landmarks, linear distances, angles, cross-sectional surface areas, and volumes at virtually any location within the craniofacial complex (Aboudara et al., 2009; Lenza et al., 2010; Ghoneima and Kula, 2013). Thus, CBCT images are useful for assessing craniofacial (dys)morphology, growth, impacted teeth, facial trauma, treatment algorithms, and bone graft outcomes (Suri et al., 2008).

The purpose of this retrospective cross-sectional study is to use 3D CBCT images to assess nasal airway volumes and septal deviation in individuals born with unilateral (i.e., right or left) or bilateral CLP. It is hypothesized that nasal airways and nasal septa will exhibit morphometric differences related to laterality and CLP type.

MATERIALS AND METHODS

CBCT images (13 cm field of view, 8.9 second scan time, 0.3 or 0.4 mm voxel size, i-Cat machine, Imaging Sciences International LLC, Hatfield, PA) were obtained for this retrospective, cross-sectional study from the Indiana University School of Dentistry (IRB approval from the Indiana University Human Subjects Office, study # 1210009813). A single CBCT image of each individual was acquired to minimized unnecessary radiation exposure. Inclusion criteria required children to be born with Veau Class III unilateral cleft lip and palate (UCLP) or Veau Class IV bilateral cleft lip and palate (BCLP) that was subsequently surgically repaired. Veau Class III and IV patients exhibit clefting of both the soft- and hard-tissues of the lip and palate, respectively. Based on these criteria (Table 1) 50 children were included in this study (left UCLP $n = 21$, right UCLP $n = 8$, BCLP $n = 21$). UCLP samples are skewed towards the left side because UCLP often exhibits a laterality preference for the left side of the face (Carroll and Mossey, 2012). Due to limitations of sample size no attempt was made to control for ancestry; however, the majority of the sample was Caucasian. Approximately 56% of these individuals previously had a primary alveolar bone graft as part of their surgical treatment algorithm. For the purposes of analysis the overall sample was divided into subsamples based on CLP type (left unilateral, right unilateral, or bilateral), age, age groups (7–9 years, 10–12 years, 13–18 years), sex (male or female), and whether individuals were previously treated with an alveolar bone graft (yes or no).

Coded CBCT images were analyzed using 3D Dolphin Imaging software (v11.5; Chatsworth, CA) and semiautomatic segmentation by the same individual (JMS) on the same computer and monitor. Orientation was standardized three-dimensionally using an

TABLE 1. Cleft Lip and Palate Sample Statistics

Cleft type	Total sample size ($N = 50$)	Total number of males ($n = 37$)	Total number of females ($n = 13$)	Mean age (years) ± standard deviation	Age range (years)	Percentage with alveolar bone graft
Left unilateral	21	17	4	11 ± 2.8	7–18	52% (11/21)
Right unilateral	8	6	2	11 ± 2.75	8–16	50% (4/8)
Bilateral	21	14	7	11 ± 3.64	7–18	62% (13/21)

orientation module in Dolphin software that positioned CBCT images in lateral view by passing a line through orbitale and porion, and in frontal view by passing a line through nasion and menton to establish the midline plane. Anatomical and constructed landmarks (Table 2) were identified on the midline sagittal CBCT image slice (Figs. 1A and 1B) to segment nasal airway sagittal boundaries and to locate the anterior nasal spine (ANS), posterior nasal spine (PNS), and midpoint of the anterior and posterior nasal spine (MNS) (Fig. 1C). Additional nasal airway boundaries were placed in coronal view (Figs. 1D and 1E) by locating crista gali and outlining nasal airway anatomy on the CBCT slice with largest nasal airway cross-sectional surface area (Fig. 1F). Dolphin software then automatically calculated anterior, middle, and posterior nasal airway volumes (sensitivity setting 60) for the right and left sides of the nasal airways using sagittal and coronal boundaries of the soft- and hard-tissue anatomy of the craniofacial complex (Table 3). Previous investigations have found that volumetric measurements from Dolphin software to be accurate and reliable (Weissheimer et al., 2012). Septal deviation was measured from CBCT slices at the level of the ANS, PNS, and the midpoint between ANS and PNS by passing a perpendicular midline through crista gali to the palatal plane in coronal view and measuring the longest distance drawn perpendicular from the midline to the deviated segment of the septum in coronal view (Table 3, Fig. 1G). Septal deviation values were recorded as negative or positive depending on whether deviation was to the right or left of the midline, respectively.

TABLE 2. Definitions of Landmarks Identified on Cone Beam Computed Tomography Image Slices

Landmark definitions
1. Rhinion (rh): most inferior and anterior point between nasal bones
2. Soft tissue pronasale (prn): the most protruded point of the apex nasi
3. Anterior nasal spine (ANS): the anterior most pointed projection of the intermaxillary suture
4. Midpoint nasal spine (MNS): midpoint of straight line whose end points are anterior nasal spine and posterior nasal spine
5. Intersection of rh-s and perpendicular line through MNS: this landmark lies on a line drawn through rhinion and sella and is found by drawing a line through MNS that is at a right angle to the line formed by ANS-PNS
6. Posterior nasal spine (PNS): the sharp posterior extremity of the nasal crest
7. Intersection of rh-s and perpendicular line through PNS: this landmark lies on a line drawn through rhinion and sella and is found by drawing a line through PNS that is at a right angle to the line formed by ANS-PNS
8. Sella turcica (s): midpoint of the depression atop the sphenoid where the pituitary gland is situated, posterior and inferior to the optic canals

All statistical testing was conducted using Minitab (v.16.1.0) or SPSS (v.20.0.0.1). To assess repeatability, volumetric and linear measurements were recorded from 10 randomly chosen coded images on two separate occasions with order randomized and at least 24 hrs. between each measurement session to avoid memory bias. The intra-class correlation (ICC) coefficient was calculated to assess intra-observer reliability across two repeatability trials and considered acceptable if $r \geq 0.90$ (Ghoneima and Kula, 2013). The technical error of measurement (TEM) was calculated for each permutation of measurement error trials to assess intra-observer error using the following equation: $\text{TEM} = \sqrt{\sum D^2/2N}$, where D was equal to the difference of measured values between two trials and N was equal to the number of individuals measured (Simpson and Henneberg, 2002). TEM was considered acceptable when the TEM value for each measurement was $\leq$5% of the mean value for that particular measurement.

After assessing reliability and TEM, nasal airway and septal deviation measurements were collected from each CBCT image with at least 24 hrs. between each measurement session. An ordination of the pooled samples was carried out using principal components analysis (PCA). PCA graphs were generated to explore patterns of multivariate variation within the data associated with CLP type (i.e., left unilateral, right unilateral, or bilateral), age groups (i.e., 7–9 years, 10–12 years, 13–18 years), voxel size (0.3 mm or 0.4 mm), sex (i.e., male or female), and whether individuals had previously received an alveolar bone graft as part of their treatment plan (i.e., yes or no). Additionally, volumetric and linear data were analyzed using a multivariate analysis of variance (MANOVA) followed by separate post-hoc ANOVA tests for independent variables showing significant effects on the dependent variables. MANOVA was used to assess the null hypothesis of the equality of multiple averages and to determine whether one or more independent variables have a significant effect on two or more dependent variables. MANOVA is capable of detecting statistical differences that may not be discovered when only using univariate statistics. The independent variables used in the MANOVA analysis were CLP type (i.e., left unilateral, right unilateral, or

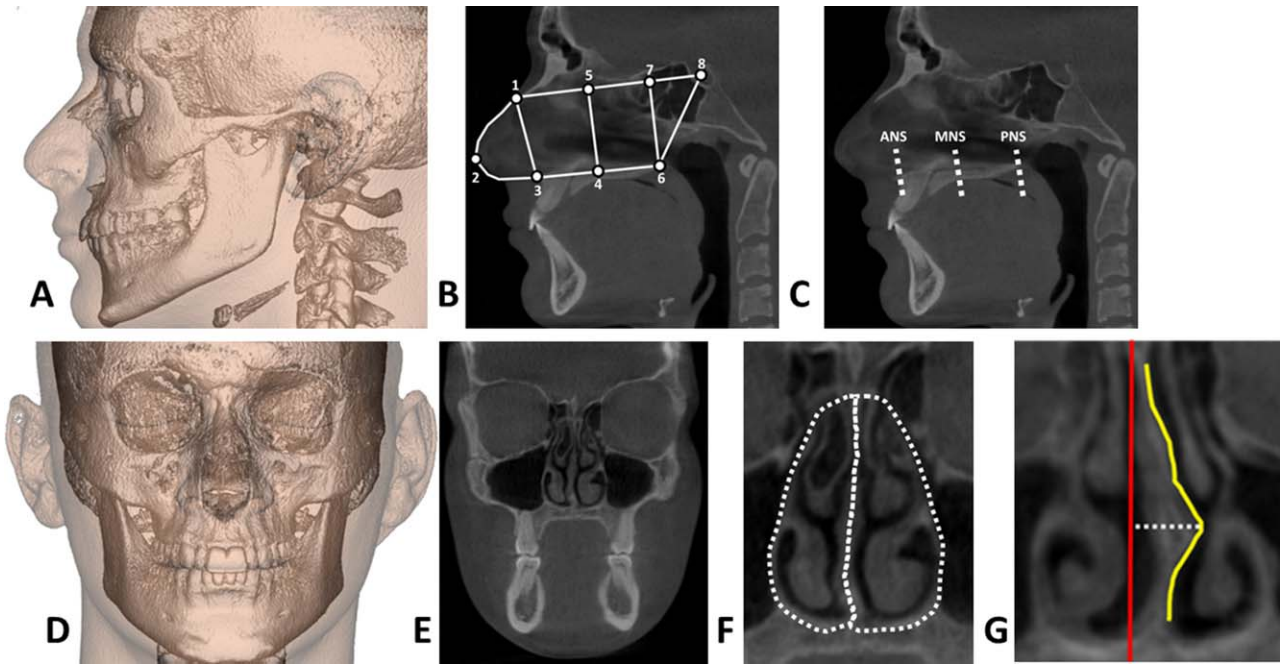

Fig. 1. Measurements collected from cone beam computed tomography (CBCT) images. **A** Sagittal view of three-dimensional CBCT image. **B** Midline sagittal CBCT slice with landmarks in place to identify the anterior (landmarks 1, 2, 3), middle (landmarks 1, 3, 4, 5), and posterior (landmarks 4, 5, 6, 7) boundaries for nasal airway volumetric measurements. **C** Locations where maximum septal deviation was measured: Anterior nasal spine (ANS), posterior nasal spine (PNS), and midpoint of anterior and posterior nasal spine (MNS). **D** Coronal view of three-dimensional CBCT. **E** Coronal CBCT slice with largest cross-sectional surface area. **F** Coronal CBCT slice outlining nasal airway boundaries for volumetric measurements. **G** Septal deviation measurement (dotted line) from the midline. [Color figure can be viewed in the online issue, which is available at wileyonlinelibrary.com.]

bilateral), age, sex (i.e., male or female), and alveolar bone graft status (i.e., yes or no). Post-hoc ANOVA tests were carried out to determine which volumetric or linear measures were significantly affected by independent variables shown to be significant by the MANOVA. Statistical significance was initially set at $P \leq 0.05$, but lowered to $P \leq 0.016$ after a Bonferonni adjustment for three tests (one MANOVA and two ANOVAs).

RESULTS

Intra-examiner reliability as assessed by ICC was high ($r = 0.98$) and indicated that volumetric and linear measurements were strongly reliable. Mean TEM for each measurement is listed in Table 4 and adequately low for all volumetric and linear measurements. Raw TEM values were higher for volumetric values since these measurements are calculated in cubic millimeters (mm^3) and, therefore, expected to have higher variances as compared to septal deviation measurements that were collected as linear distances in millimeters (mm). Mean nasal volume and septal deviation values were divided by age groups and cleft type (Table 4). Unilateral CLP nasal volumes tend to be reduced on the clefted side of the face (Table 4).

A PCA for the entire pooled sample of right unilateral, left unilateral, and bilateral CLP individuals of all ages revealed that axes 1 and 2 together explain 78.3% of the variance in the samples. Individuals partially separate based on age groups along PCA axis 1 (Fig. 2A), which explains 48.5% of variance in the samples. Nasal volume measurements are weighted more heavily than septal deviation measurements along axis 1 due to increases in nasal airway volume (and therefore size) as individuals age (Fig. 2A). Unilateral CLP individuals separate based on cleft type along axis 2 (Fig. 2B), which explains 29.82% of variance in the samples. Bilateral CLP individuals overlap with both unilateral CLP samples along axis 2. All three septal deviation measurements were weighted more heavily than volumetric measures along axis 2. Septa tend to deviate towards the clefted side of the face in unilateral CLP individuals (Choi et al., 2013), but deviate to either side in bilateral CLP individuals (Fig. 2B). This explains why unilateral CLP samples separate along axis 2 and why the bilateral CLP overlaps with both unilateral CLP samples. Additional PCA plots of axis 1 and 2 revealed no separation of individuals based on voxel size, sex, or bone graft status.

Scatterplots and regression lines were generated for nasal airway volume and septal deviation measures

TABLE 3. Nasal Airway Volume and Septal Deviation Linear Distance Measurement Definitions

Measurements	Measurement definitions
Volumes	
Anterior nasal airway (L and R)	The sagittal boundary was placed as seen in Figure 1B using landmarks 1, 2, and 3. The coronal view was placed by placing a point at crista gali and following the anatomical boundaries of the nasal septum and nasal borders. For all volume measurements, after boundaries were defined Dolphin software was used to automatically calculate volume in mm^3
Middle nasal airway (L and R)	The sagittal boundary was placed as seen in Figure 1B using landmarks 1, 3, 4, and 5. The coronal view was placed by placing a point at crista gali and following the anatomical boundaries of the nasal septum and nasal borders. Volume was calculated in mm^3
Posterior nasal airway (L and R)	The sagittal boundary was placed as seen in Figure 1B using landmarks 4, 5, 6, and 7. The coronal view was placed by placing a point at crista gali and following the anatomical boundaries of the nasal septum and nasal borders. Volume was calculated in mm^3
Linear distances	
Septal deviation at anterior nasal spine (L or R)	The coronal CBCT slice to measure was determined by locating the anterior nasal spine in sagittal view as shown in Figure 1C and switching to the coronal CBCT slice containing this anatomical location. In coronal view the deviation of the septum to the midline was measured in mm using a horizontal linear distance as depicted in Figure 1G. For all septal deviation measures, the midline was defined when image orientation was standardized in Dolphin by passing a midline through nasion and menton
Septal deviation at midpoint of anterior and posterior nasal spine (L or R)	The coronal CBCT slice to measure was determined by locating the midpoint of the anterior nasal spine and posterior nasal spine in sagittal view as shown in Figure 1C and switching to the coronal CBCT slice containing this anatomical location. In coronal view the deviation of the septum to the midline was measured in mm using a horizontal linear distance as depicted in Figure 1G
Septal deviation at posterior nasal spine (L or R)	The coronal CBCT slice to measure was determined by locating the posterior nasal spine in sagittal view as shown in Figure 1C and switching to the coronal CBCT slice containing this anatomical location. In coronal view the deviation of the septum to the midline was measured in mm using a horizontal linear distance as depicted in Figure 1G

Landmark definitions are provided in Table 2.

(Fig. 3). Airway volume increases with age in the anterior, middle, and posterior regions of the nasal airway (Figs. 3A and 3B). Septal deviation remains consistent at MNS and increases slightly with age at ANS and PNS (Fig. 3C) with maximal septal deviation occurring at PNS at the time of full facial maturity (Friel et al., 2013). A MANOVA revealed a significant multivariate main effect for CLP type ($P \leq 0.001$) and age ($P = 0.007$) (Table 5). These results confirm the hypothesis that CLP type (i.e. right unilateral, left unilateral, and bilateral) and age have significant effects on nasal airway volume and septal deviation values. Given the significance of the overall MANOVA test, the univariate main effects were examined with post-hoc ANOVA tests. Significant univariate main effects for age were obtained for right anterior nasal volume ($P \leq 0.001$) and left anterior nasal volume ($P \leq 0.001$), whereas left posterior nasal volume ($P = 0.048$) and septal deviation at MNS ($P = 0.04$) only approached significance after a Bonferonni adjustment to $\alpha \leq 0.016$ (Table 5). Significant univariate main effects for cleft type were obtained for septal deviation at ANS ($P \leq 0.01$), septal deviation at MNS ($P \leq 0.01$), septal deviation at PNS ($P \leq 0.01$), and right posterior nasal volume ($P = 0.014$), whereas right middle nasal volume ($P = 0.04$) only approached significance after a Bonferonni correction (Table 5).

DISCUSSION

CLP is associated with a variety of anatomical and physiological craniofacial impairments, including nasal airway obstruction (Suzuki et al., 1999). The multivariate relationships between age, CLP types (i.e., unilateral and bilateral), nasal airway volume, and septal deviation laterality have rarely been investigated. Recent advances in three-dimensional (3D) imaging such as the development of CBCT and 3D visualization software allow researchers to quantitatively measure virtually any aspect of the craniofacial complex (Suri et al., 2008; Ghoneima and Kula, 2013).

A PCA was carried out as an ordination method to explore multivariate patterns of variation in high-dimensional space (Fig. 2). Principal component axis 1 (PC1) explains 48.5% of the variance in pooled CLP samples. CLP individuals partially separate along PC1 based on the following age groupings: (a) 7–9 years, (b) 10–12 years, and (c) 13–18 years. Nasal volume measurements are most heavily weighted along PC1. Taken together, this evidence suggests that both internal and external nasal airway volumes tend to increase in individuals born with CLP and therefore, nasal airway obstruction may be reduced as faces develop and mature.

Principal component axis 2 (PC2) explains 29.8% of variance in pooled CLP samples. Individuals born

TABLE 4. Technical Error of Measurement (TEM), Mean Septal Deviation, and Mean Nasal Volume Measurements Divided by Maturity and Cleft Type

	Mean TEM	7–9 years	10–12 years	13–18 years	Left unilateral	Right unilateral	Bilateral
Mean septal deviation at the anterior nasal spine (absolute value) (mm)	0.04	4.72	4.09	5.16	4.24	4.65	5.18
Mean septal deviation at the midpoint of the anterior and posterior nasal spine (absolute value) (mm)	0.05	5.29	4.76	5.95	4.98	5.98	5.73
Mean septal deviation at the posterior nasal spine (absolute value) (mm)	0.04	5.26	4.34	5.35	4.69	5.63	5.41
Mean right anterior nasal volume (mm^3)	42.9	1,318.01	1,626.92	3,006.56	2,046.95	1,427.96	1,915.1
Mean right middle nasal volume (mm^3)	66.48	2,041.25	2,768.15	3,855.43	2,984.21	2,424.7	2,628.8
Mean right posterior nasal volume (mm^3)	81.68	2,876.16	3,960.13	5,307.28	3,986.05	3,841.84	3,702.7
Mean left anterior nasal volume (mm^3)	49.77	1,390.27	1,903.64	3,098.68	1,726.92	2,071.96	1,883.12
Mean left middle nasal volume (mm^3)	67.89	1,704.05	2,445.08	4,101.50	2,842.83	2,682.14	2,293.29
Mean left posterior nasal volume (mm^3)	77.95	2,108.65	3,449.05	5,448.07	3,638.69	3,923.41	2,974.7

with unilateral CLP completely separate along this axis, while individuals born with bilateral CLP overlap with both unilateral CLP samples. All three measures of maximum septal deviation (i.e., at ANS, MNS, and PNS) are weighted most heavily along axis 2. This result is likely due to the fact that septal deviation values were recorded as negative or positive values depending on whether they deviated towards the right or left side, respectively. We found that septa typically deviate towards the affected side in UCLP. Nasal septa

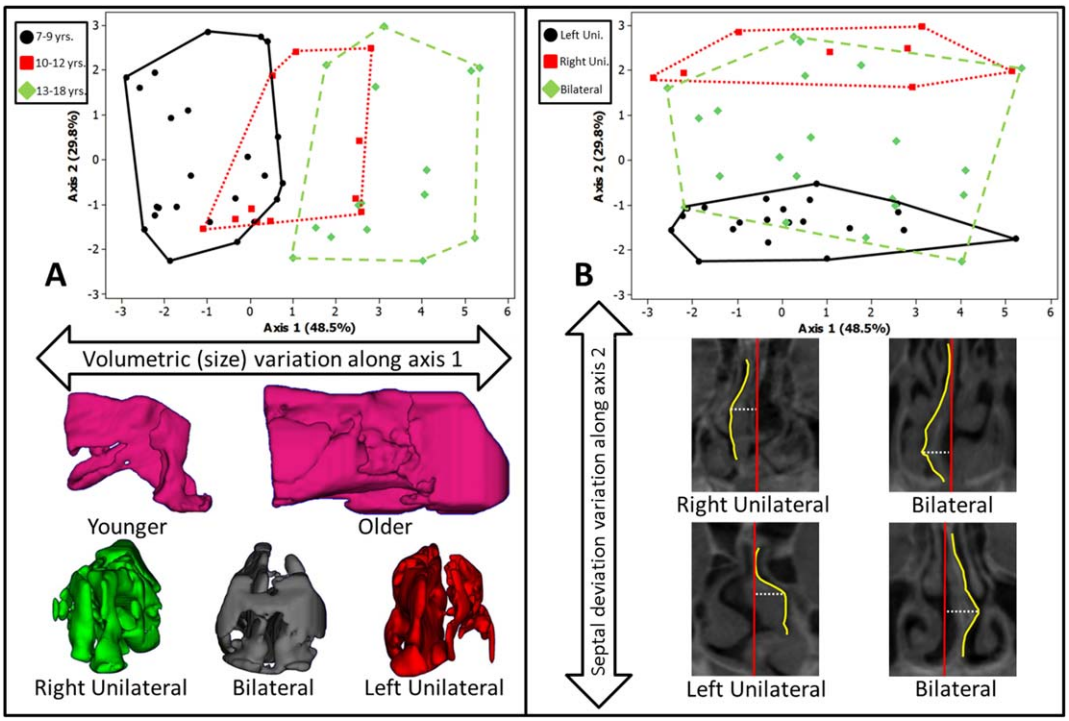

Fig. 2. Principal components analysis (PCA) results. **A** Principal component axis 1 (PC1) explains 48.5% of the variance among samples. Anterior, middle, and posterior nasal airway volume measures are loaded heavily along PC1, and samples partially separate based on 7–9 years (solid lines), 10–12 years (dotted lines), and 13–18 years (dashed lines) age groupings. Lateral nasal airway reconstructions are depicted for younger and older extremes to illustrate variation across age groups. Anterior nasal airway reconstructions are depicted to illustrate variation across cleft lip and palate (CLP) types (i.e., right unilateral, left unilateral, bilateral). **B** Samples separate based on CLP type along PC2, which explains 29.8% of the variance among samples. Nasal septa tend to deviate towards the clefted side of the face in unilateral CLP individuals, and deviate in either direction in bilateral CLP individuals. [Color figure can be viewed in the online issue, which is available at wileyonlinelibrary.com.]

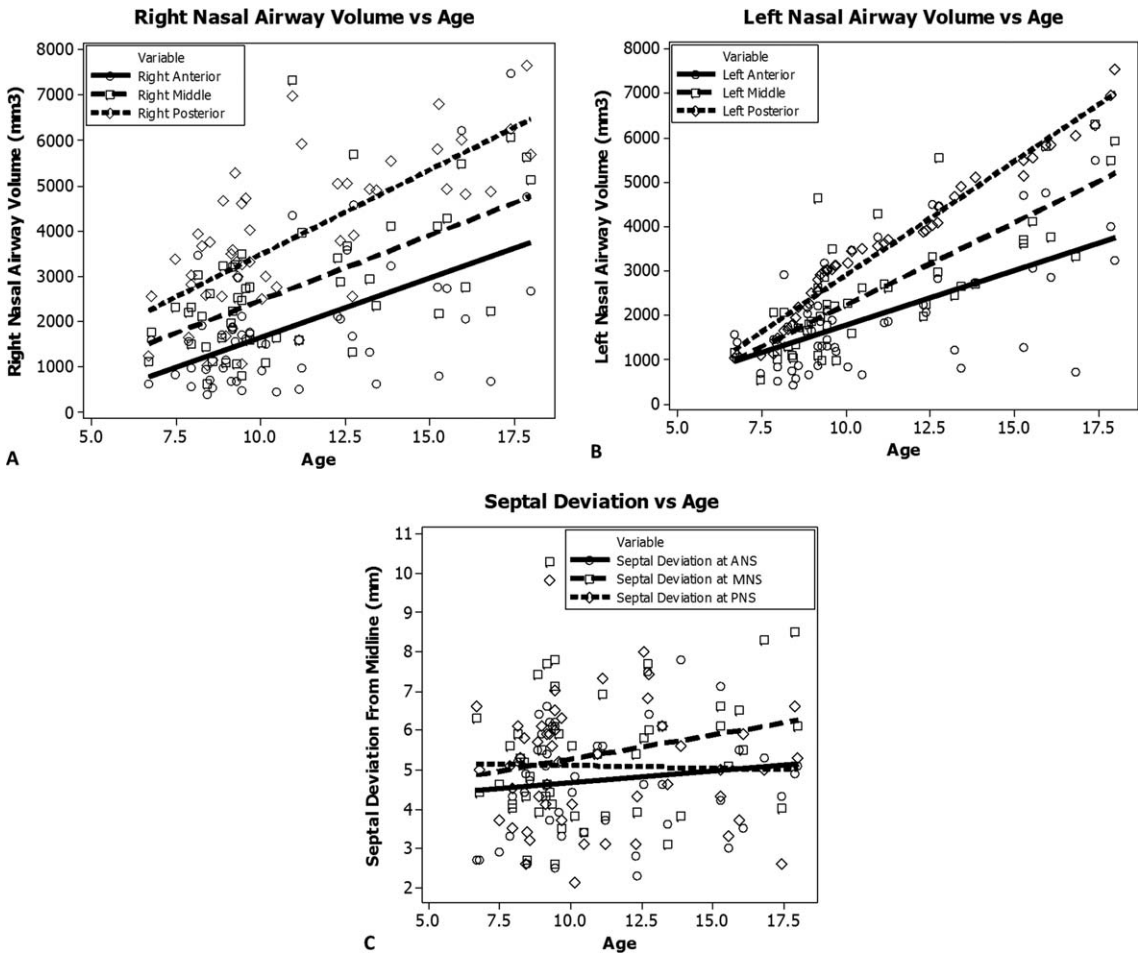

Fig. 3. Scatterplots and regression lines for pooled nasal airway volume and septal deviation values plotted against age. **A** Right anterior (circles, solid regression line), middle (squares, dashed regression line), and posterior (diamonds, square dot regression line) nasal airway volume plotted against age. **B** Left anterior (circles, solid regression line), middle (squares, dashed regression line), and posterior (diamonds, square dot regression line) nasal airway volume plotted against age. **C** Maximum septal deviation at anterior nasal spine (ANS; circles, solid regression line), the midpoint of anterior and posterior nasal spine (MNS; squares, dashed regression line), and posterior nasal spine (PNS; diamonds, square dot regression line) plotted against age.

deviate toward either the right or left side in individuals born with BCLP, and this is why the bilateral CLP sample overlaps with both unilateral CLP samples along PC2. These results indicate that nasal septa deviation is strongly associated with CLP type and support previous observations that septa deviate towards the clefted side of the face in individuals born with UCLP (Molsted and Dahl, 1990; Kolbenstvedt et al., 2002; Suri et al., 2008; Carroll and Mossey, 2012).

Although 56% of individuals included in this study had previously been treated with alveolar bone grafts, a MANOVA test for the effects of this treatment failed to reach statistical significance. MANOVA testing for effects based on sex also failed to reach statistical significance; however, approximately half of the children included in this study were likely pre-pubescent and, therefore, had not yet developed sexually dimorphic characteristics associated with puberty.

Anterior, middle, and nasal airway volumes tend to be reduced on the clefted side of the face of individuals born with UCLP (Table 4). Scatterplots and regression lines indicate that nasal airway volume tends to greatly increase as faces grow whereas septal deviation measurements change slightly (Fig. 3). It is notable that the most deviated area of the nasal septum at the time of facial maturity is at the PNS, an area commonly overlooked by rhinoplasty surgeons when correcting septal deviation (Friel et al., 2013). MANOVA results indicate that age ($P = 0.007$) and CLP type (i.e., right unilateral, left unilateral, and bilateral; $P \leq 0.001$) significantly affect nasal airway volume and septal deviation values (Table 5). ANOVA results indicate that measurements affected by age include right and left anterior nasal volume, left posterior nasal volume, and septal deviation at MNS. However, only anterior nasal volume measures remain significant

TABLE 5. MANOVA and ANOVA Results

MANOVA results					
Effect		Value	*F*	*P* value	Observed power
CLP type	Wilks' Lambda	0.139	4.68	≤0.001	1.000
Age	Wilks' Lambda	0.027	1.578	0.007	0.989
ANOVA results					
			F	*P* value	Observed power
Age	Right anterior NAV		4.732	≤0.001	0.994
	Left anterior NAV		4.744	≤0.001	0.996
	Left posterior NAV		2.2	0.048	0.797
	Sept. Dev. at MNS		2.295	0.04	0.818
CLP type	Right middle NAV		3.556	0.04	0.62
	Right posterior NAV		4.827	0.014	0.761
	Sept. Dev. at ANS		12.936	≤ 0.001	0.995
	Sept. Dev. at MNS		25.595	≤ 0.001	1.000
	Sept. Dev. at PNS		23.492	≤ 0.001	1.000

MANOVA results show a significant multivariate main effect for cleft lip and palate (CLP) type (i.e., right unilateral, left unilateral, or bilateral) and age on measurements of anterior, middle, and posterior nasal airway volume (NAV), and septal deviation (Sep. Dev.) at the anterior nasal spine (ANS), posterior nasal spine (PNS), and midpoint of the anterior and posterior nasal spines (MNS). ANOVA results show significant univariate main effects for CLP type and age for different NAV and Sep. Dev. measures. Due to multiple testing a Bonferonni correction was employed and the *P* value was adjusted (≤0.016).

($P \leq 0.001$) after a correction for multiple tests (Table 5). Taken together, these results suggest that anterior nasal growth increases volume of the nasal airway significantly as faces affected by CLP mature. This result is supported by a previous investigation where nasal airway volume was found to scale isometrically (i.e., positively covaries) with facial size (Butaric et al., 2010) and another investigation which found that nasal growth velocity is maximized around 11–13 years of age although nasal growth continues as faces mature (van der Heijden et al., 2008).

Additionally, ANOVA results indicate that measurements affected by CLP type include right middle and right posterior nasal volume, and septal deviation at ANS, MNS, and PNS. After Bonferonni correction, only septal deviation at ANS ($P \leq 0.001$), MNS ($P \leq 0.001$), and PNS ($P \leq 0.001$) remain significant (Table 5). The absolute amount of septal deviation is similar across individuals born with UCLP and BCLP (Table 4).

One function of the nasal complex is to adjust the temperature and humidity of respired air, which protects the alveolar membranes from thermal injury and keeps the nasal membrane wet to facilitate oxygen absorption and carbon dioxide excretion (Yokley, 2009). Individuals born with CLP often suffer from nasal airway obstruction, deviated nasal septa, turbinate hypertrophy, rhinosinusitis, and external nasal deformities, and all of these factors can impair nasal respiration (Suzuki et al., 1999). In biomechanical terms, the nasal septum and walls of the nasal cavity have been described as framing elements that are adapted to the mechanical and functional demands of the craniofacial complex by functioning to resist masticatory forces transmitted through the dentition to the palate and maxilla (Badoux, 1966). It has been argued that nasal airway shape is a response to respiratory demands because nasal turbinate size covaries with nasal airway shape even when nasal airways are reduced due to congenital anomalies (Chierici et al., 1973b).

Although we found reduced nasal airway volumes and nasal septa deviation patterns specific to CLP type (i.e., left unilateral, right unilateral, bilateral), it is not possible to determine if these craniofacial dysmorphologies occurred due to inadequate spatiotemporal and morphogenetic developmental mechanisms or if these dysmorphologies are simply developmentally plastic adaptational responses to abnormal structures derived from perturbed morphogenetic developmental events (Harvold, 1953; Chierici et al., 1973a; Molsted and Dahl, 1990). However, reduced airway size on the clefted side of the face suggests that functional nasal breathing may be impaired in individuals born with CLP despite multiple surgeries aimed at aesthetic restoration of soft-tissue facial features. Additionally, traditional septoplasty only addresses the cartilaginous septum, which only encompasses the anterior half of the nasal septum. In order to provide complete restoration to nasal airflow, septal surgery should also include restoration of the posterior septum, an area comprised mostly of bone (Friel et al., 2013).

We note that although we have found significant changes in nasal airway volume and septal deviation in patients with CLP, we have not correlated these findings with a functional analysis of airflow. The direct effects of these anatomic findings on nasal airflow will be the topic of future studies. Furthermore, all patients in this study had CLP. It is certainly possible that patients with cleft lip only and an intact hard palate may exhibit different patterns of nasal airway and septal deviation and, thus, our findings should be limited to the CLP population.

Previous investigations have suggested that bony septum deviation may be a response to maxillary sinus deformation (Chierici et al., 1973a, b); however, these studies were carried out using 2D cephalograms and therefore unable to truly quantify the three-dimensional relationship between maxillary sinus volume and septal deviation. Thus, future research should assess the maxillary sinuses of individuals born with CLP using 3D

imaging to determine the associations between maxillary pneumatization, CLP, and septal deviation.

ACKNOWLEDGMENTS

We would like to thank two anonymous reviewers who provided thoughtful comments and suggestions to improve this manuscript. This work was supported by the Indiana University-Purdue University Indianapolis (IUPUI) Signature Center Initiative-Three Dimensional Imaging of the Craniofacial Complex Center (3D ICCC) and a Jarabak Endowed Professorship. The content of this manuscript is solely the responsibility of the authors and does not necessarily represent the official views of these funding sources.

REFERENCES

Aboudara C, Nielsen I, Huang JC, Maki K, Miller AJ, Hatcher D. 2009. Comparison of airway space with conventional lateral headfilms and 3-dimensional reconstruction from cone-beam computed tomography. Am J Orthod Dentofacial Orthop 135: 468–479.

Agarwal R, Parihar A, Mandhani PA, Chandra R. 2012. Three-dimensional computed tomographic analysis of the maxilla in unilateral cleft lip and palate: Implications for rhinoplasty. J Craniofac Surg 23:1338–1342.

Attanasio C, Nord AS, Zhu Y, Blow MJ, Li Z, Liberton DK, Morrison H, Plajzer-Frick I, Holt A, Hosseini R, Phouanenavong S, Akiyama JA, Shoukry M, Afzal V, Rubin EM, FitzPatrick DR, Ren B, Hallgrimsson B, Pennacchio LA, Visel A. 2013. Fine tuning of craniofacial morphology by distant-acting enhancers. Science 342: 1241006.

Badoux DM. 1966. Framed structures in the mammalian skull. Acta Morphol Neerl Scand 6:239–250.

Bell A, Lo TW, Brown D, Bowman AW, Siebert JP, Simmons DR, Millett DT, Ayoub AF. 2013. Three-dimensional assessment of facial appearance following surgical repair of unilateral cleft lip and palate. Cleft Palate Craniofac J.

Brugmann SA, Kim J, Helms JA. 2006. Looking different: Understanding diversity in facial form. Am J Med Genet A 140: 2521–2529.

Bugaighis I, Mattick CR, Tiddeman B, Hobson R. 2013. 3D asymmetry of operated children with oral clefts. Orthod Craniofac Res.

Butaric LN, McCarthy RC, Broadfield DC. 2010. A preliminary 3D computed tomography study of the human maxillary sinus and nasal cavity. Am J Phys Anthropol 143:426–436.

Carroll K, Mossey PA. 2012. Anatomical Variations in Clefts of the Lip with or without Cleft Palate. Plast Surg Int 2012:542078.

Chierici G, Harvold EP, Vargervik K. 1973a. Morphogenetic experiments in cleft palate: Mandibular response. Cleft Palate J 10: 51–61.

Chierici G, Harvold EP, Vargervik K. 1973b. Morphogenetic experiments in facial asymmetry: The nasal cavity. Am J Phys Anthropol 38:291–299.

Choi YK, Park SB, Kim YI, Son WS. 2013. Three-dimensional evaluation of midfacial asymmetry in patients with nonsyndromic unilateral cleft lip and palate by cone-beam computed tomography. Korean J Orthod 43:113–119.

Farkas LG, Posnick JC, Hreczko TM. 1992. Growth patterns of the face: A morphometric study. Cleft Palate Craniofac J 29: 308–315.

Feng W, Leach SM, Tipney H, Phang T, Geraci M, Spritz RA, Hunter LE, Williams T. 2009. Spatial and temporal analysis of gene expression during growth and fusion of the mouse facial prominences. PLoS One 4:e8066.

Ferrario VF, Sforza C, Poggio CE, Schmitz JH. 1998. Craniofacial growth: A three-dimensional soft-tissue study from 6 years to adulthood. J Craniofac Genet Dev Biol 18:138–149.

Freeman AK, Mercer NS, Roberts LM. 2013. Nasal asymmetry in unilateral cleft lip and palate. J Plast Reconstr Aesthet Surg 66: 506–512.

Friel MT, Starbuck JM, Ghoneima AM, Murage K, Kula KS, Tholpady S, Havlik RJ, Flores RL. 2013. Airway Obstruction and the Unilateral Cleft Lip and Palate Deformity: Contributions by the Bony Septum. Ann Plast Surg.

Ghoneima A, Kula K. 2013. Accuracy and reliability of cone-beam computed tomography for airway volume analysis. Eur J Orthod 35:256–261.

Gregg JB, Zimmerman L, Clifford S, Gregg PS. 1981. Craniofacial anomalies in the Upper Missouri River over a millennium: Archeological and clinical evidence. Cleft Palate J 18:210–222.

Hall BK, Precious DS. 2013. Cleft lip, nose, and palate: The nasal septum as the pacemaker for midfacial growth. Oral Surg Oral Med Oral Pathol Oral Radiol 115:442–447.

Harvold EP. 1953. Cleft lip and palate: Morphologic studies of the facial skeleton. In: 24th Annual Meeting of the Great Lakes Society of Orthodontists. Grand Rapids, Michigan. p 493–506.

Hasanzadeh N, Majidi MR, Kianifar H, Eslami N. 2014. Facial soft-tissue morphology of adolescent patients with nonsyndromic bilateral cleft lip and palate. J Craniofac Surg 25:314–317.

Jena AK, Singh SP, Utreja AK. 2011. Effects of sagittal maxillary growth hypoplasia severity on mandibular asymmetry in unilateral cleft lip and palate subjects. Angle Orthod 81:872–877.

Jiang R, Bush JO, Lidral AC. 2006. Development of the upper lip: Morphogenetic and molecular mechanisms. Dev Dyn 235: 1152–1166.

Klimentidis YC, Shriver MD. 2009. Estimating genetic ancestry proportions from faces. PLoS One 4:e4460.

Kolbenstvedt A, Aalokken TM, Arctander K, Johannessen S. 2002. CT appearances of unilateral cleft palate 20 years after bone graft surgery. Acta Radiol 43:567–570.

Lee JK, Park JW, Kim YH, Baek SH. 2012. Association between PAX9 single-nucleotide polymorphisms and nonsyndromic cleft lip with or without cleft palate. J Craniofac Surg 23:1262–1266.

Lenza MG, Lenza MM, Dalstra M, Melsen B, Cattaneo PM. 2010. An analysis of different approaches to the assessment of upper airway morphology: A CBCT study. Orthod Craniofac Res 13:96–105.

Marazita ML. 2012. The evolution of human genetic studies of cleft lip and cleft palate. Annu Rev Genomics Hum Genet 13:263–283.

Molsted K, Dahl E. 1990. Asymmetry of the maxilla in children with complete unilateral cleft lip and palate. Cleft Palate J 27:184–190; discussion 190–182.

Ras F, Habets LL, van Ginkel FC, Prahl-Andersen B. 1994. Three-dimensional evaluation of facial asymmetry in cleft lip and palate. Cleft Palate Craniofac J 31:116–121.

Ras F, Habets LL, van Ginkel FC, Prahl-Andersen B. 1995. Longitudinal study on three-dimensional changes of facial asymmetry in children between 4 to 12 years of age with unilateral cleft lip and palate. Cleft Palate Craniofac J 32:463–468.

Schendel SA, Hatcher D. 2010. Automated 3-dimensional airway analysis from cone-beam computed tomography data. J Oral Maxillofac Surg 68:696–701.

Seidenstricker-Kink LM, Becker DB, Govier DP, DeLeon VB, Lo LJ, Kane AA. 2008. Comparative osseous and soft tissue morphology following cleft lip repair. Cleft Palate Craniofac J 45:511–517.

Simpson E, Henneberg M. 2002. Variation in soft-tissue thicknesses on the human face and their relation to craniometric dimensions. Am J Phys Anthropol 118:121–133.

Son WS. 1995. Facial Asymmetry of Unilateral Cleft Lip and Palate Patients. Korea J. Orthod 25:13–18.

Starbuck JM, Ward RE. 2007. The affect of tissue depth variation on craniofacial reconstructions. Forensic Sci Int 172:130–136.

Suri S, Utreja A, Khandelwal N, Mago SK. 2008. Craniofacial computerized tomography analysis of the midface of patients with repaired complete unilateral cleft lip and palate. Am J Orthod Dentofacial Orthop 134:418–429.

Suzuki H, Yamaguchi T, Furukawa M. 1999. Rhinologic computed tomographic evaluation in patients with cleft lip and palate. Arch Otolaryngol Head Neck Surg 125:1000–1004.

Thomason H, Dixon M. 2009. Craniofacial Defects and Cleft Lip and Palate. In: Encyclopedia of Life Sciences (ELS). Chichester: John Wiley & Sons.

Trindade-Suedam IK, da Silva Filho OG, Carvalho RM, de Souza Faco RA, Calvo AM, Ozawa TO, Trindade AS, Jr., Trindade IE. 2012. Timing of alveolar bone grafting determines different outcomes in patients with unilateral cleft palate. J Craniofac Surg 23:1283–1286.

Tso HH, Lee JS, Huang JC, Maki K, Hatcher D, Miller AJ. 2009. Evaluation of the human airway using cone-beam computerized tomography. Oral Surg Oral Med Oral Pathol Oral Radiol Endod 108:768–776.

van der Heijden P, Korsten-Meijer AG, van der Laan BF, Wit HP, Goorhuis-Brouwer SM. 2008. Nasal growth and maturation age in adolescents: A systematic review. Arch Otolaryngol Head Neck Surg 134:1288–1293.

Weinberg SM, Naidoo SD, Bardi KM, Brandon CA, Neiswanger K, Resick JM, Martin RA, Marazita ML. 2009. Face shape of unaffected parents with cleft affected offspring: Combining three-dimensional surface imaging and geometric morphometrics. Orthod Craniofac Res 12:271–281.

Weissheimer A, Menezes LM, Sameshima GT, Enciso R, Pham J, Grauer D. 2012. Imaging software accuracy for 3-dimensional analysis of the upper airway. Am J Orthod Dentofacial Orthop 142:801–813.

Yokley TR. 2009. Ecogeographic variation in human nasal passages. Am J Phys Anthropol 138:11–22.

Young DL, Schneider RA, Hu D, Helms JA. 2000. Genetic and teratogenic approaches to craniofacial development. Crit Rev Oral Biol Med 11:304–317.

Young NM, Hu D, Lainoff AJ, Smith FJ, Diaz R, Tucker AS, Trainor PA, Schneider RA, Hallgrimsson B, Marcucio RS. 2014. Embryonic bauplans and the developmental origins of facial diversity and constraint. Development 141:1059–1063.